

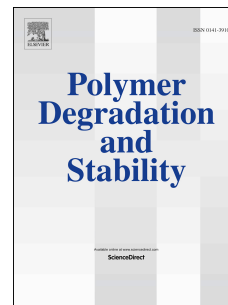
This is the Post-print version of the following article: *Jahell Alvarado, Guillermo Acosta, Fatima Perez, Study of the effect of the dispersion of functionalized nanoparticles TiO₂ with photocatalytic activity in LDPE, Polymer Degradation and Stability, Volume 134, 2016, Pages 376-382*, which has been published in final form at: <https://doi.org/10.1016/j.polymdegradstab.2016.11.009>

© 2016. This manuscript version is made available under the CC-BY-NC-ND 4.0 license <http://creativecommons.org/licenses/by-nc-nd/4.0/>

Accepted Manuscript

Study of the effect of the dispersion of functionalized nanoparticles TiO₂ with photocatalytic activity in LDPE

Alvarado Jahell, Acosta Guillermo, Perez Fatima



PII: S0141-3910(16)30344-5

DOI: [10.1016/j.polymdegradstab.2016.11.009](https://doi.org/10.1016/j.polymdegradstab.2016.11.009)

Reference: PDST 8107

To appear in: *Polymer Degradation and Stability*

Received Date: 20 September 2016

Revised Date: 5 November 2016

Accepted Date: 6 November 2016

Please cite this article as: Jahell A, Guillermo A, Fatima P, Study of the effect of the dispersion of functionalized nanoparticles TiO₂ with photocatalytic activity in LDPE, *Polymer Degradation and Stability* (2016), doi: 10.1016/j.polymdegradstab.2016.11.009.

This is a PDF file of an unedited manuscript that has been accepted for publication. As a service to our customers we are providing this early version of the manuscript. The manuscript will undergo copyediting, typesetting, and review of the resulting proof before it is published in its final form. Please note that during the production process errors may be discovered which could affect the content, and all legal disclaimers that apply to the journal pertain.

1 **Study of the effect of the dispersion of functionalized nanoparticles TiO₂ with photocatalytic**
2 **activity in LDPE**

3 Alvarado Jahell¹, Acosta Guillermo², Perez Fatima^{3*}

4
5 ¹Nanotechnology Incubator I²T², Apodaca, Nuevo León, Mexico Zip Code 66629.

6 ²NANOMATERIALES SA de CV, San Pedro Garza Garcia, Nuevo Leon, Mexico. Zip Code 66269.

7 ³CONACYT -The Institute for Scientific and Technological Research of San Luis Potosi, Mexico. Zip Code 78216.

8 *Corresponding author at: CONACYT -The Institute for Scientific and Technological

9 Research of San Luis Potosi, Mexico Tel+524448342000.

10 E-mail: fatima.perez@ipicyt.edu.mx

11
12 **ABSTRACT**

13 A photodegradable Low Density Polyethylene-Titanium dioxide (LDPE-TiO₂) nanocomposite film was
14 prepared, and its evaluation considers the partial modification of the surface of the particle using
15 Hexadecyltrimethoxysilane (HDTMS) as functionalizing agent under Ultraviolet (UV) radiation. Reaction
16 efficiency of the nanoparticles was evaluated with Thermogravimetric (TGA) and infrared analysis (FT-
17 IR). Nanocomposites were prepared by a melt blending technique; using a twin-screw extruder, each
18 nanocomposite film was thermoformed into different shapes for further evaluation. Scanning Electron
19 Microscopy (SEM) was utilized to determine the size and distribution of nanoparticles in the polymer.
20 Experimental results indicate that surface modification increases the degree of dispersion while
21 decreasing the particle size, enhancing the particle's compatibility with the polymer matrix.
22 Photocatalytic degradation was assessed through accelerated degradation weathering in a chamber under
23 UV radiation to assess the performance of photocatalytic degradation. These tests indicated, that the
24 particle's homogeneity of dispersion and size reduction by functionalization allows for homogeneously
25 degraded surfaces (SEM) to generated a greater abundance of oxidized groups in the sample compared
26 with unfunctionalized sample.

27 **Keywords:** Titanium dioxide, nanocomposite, photocatalytic, functionalization.

28 **1. Introduction**

29 Waste accumulation is a problem that many researchers are addressing in order to reduce it due to its
30 negative impact on the environment. In recent years, advanced materials have demonstrated valuable
31 properties in waste management. Polymers constitute an important proportion of global waste;

32 polyethylene is frequently used in the packaging industry [1,2], which causes waste accumulation due to
33 its high resistance to degradation [3]. There are several ways to degrade wasted polymeric materials
34 rapidly. Thermal degradation is one method; however, it produces highly toxic volatile materials such as
35 methane, aldehydes and ketones [4]; and is therefore, it is not suited as a remedy for pollution polymers.
36 A different approach lies in creating polymer compounds with degradable biological materials; however,
37 in this process, the microorganisms consume the biological material, leaving non-degradable material in
38 the environment. Heterogeneous photocatalytic degradation as a third alternative permits nanomaterials to
39 generate compounds degradable by UV radiation, and has been investigated for waste-water and
40 drinking-water treatment [5,6].

41 Heterogeneous photocatalysis is an Advanced Oxidation Technology (AOT) that involves the formation
42 of an electron-hole pair by energy absorption (UV). This pair reacts with the organic substrate and hereby
43 forms free radicals that increase in the concentration of oxygen-containing groups, such as peroxides,
44 hydroperoxides, and also the ketonic carbonyl groups [7–9]. Materials such as Titanium dioxide (TiO₂)
45 and Zinc Oxide (ZnO) are often utilized due to their excellent photocatalytic properties, low toxicity, and
46 high oxidative activity [10,11]. Thus, these materials are frequently incorporated into different materials
47 to add antibacterial [12–14], odor-inhibition, and self-cleaning properties. When employed at nanometer
48 size, these properties are enhanced because of greater surface-volume portion [11,15].

49 However, nanoparticles must be supported on a matrix to avoid secondary recovery processes after
50 photocatalytic degradation in polymers [16,17]. Furthermore, complete degradation of waste material
51 requires sufficient contact time between the matrix and the particles; therefore, the particles must remain
52 anchored sufficiently long to achieve a uniform oxidative process. In this way, if the nanoparticles are not
53 properly anchored to the substrate, they may eventually migrate to the surface and diffuse as inhalable
54 toxic powder [8,18].

55 Kamrannejad et al. proposes that photocatalytic process of crosslinking and chain breakage be
56 predominant reactions of the degradation of thermoplastics such as polyethylene and polypropylene. This
57 is determined by evaluating the mechanical properties of the nanocomposite, in which the elastic modulus
58 increases while elongation decreases upon exposure to UV radiation [19]. Additionally Moghaddam et al.
59 propose that the mechanical properties of nanocomposites depend directly on the distribution and size of
60 the agglomerates formed [2].

61 Because nanoparticles usually stick together to form agglomerates of the size of some microns with
62 increased hydrophilic character (high surface hydroxyl groups), these become incompatible with
63 polymers; thus, migration to the surface occurs, losing the photocatalytic activity [20,21].

64 Other studies have demonstrated that degradation caused by TiO_2 is directly related with its concentration
65 [8]. In addition to concentration, photocatalytic degradation depends on particle size, in which activity is
66 enhanced by reducing the particle's diameter [4]. Considering that adequate nanoparticle size and
67 distribution in a polymer matrix is fundamental for photocatalytic degradation and that the
68 functionalization process will result in proper dispersion of nanoparticles in the polymer matrix, which
69 lowers surface energy without compromising photocatalytic performance, this paper presents the results
70 of the photocatalytic activity of the partial functionalization of Titanium dioxide nanoparticles and their
71 incorporation into a polymer matrix of Low Density Polyethylene (LDPE) by extrusion. The variables
72 analyzed include particle-size distribution in the polymer matrix and photocatalytic performance in the
73 presence of UV radiation.

74 **2. Materials and Methods**

75 2.1 Materials

76 Titanium dioxide (TiO_2) nanoparticles were provided by Degussa P25 (70% in Anatase and 30% Rutile
77 phase), with primary particle diameters within the range of 30-50 nm. Ethyl alcohol, ACS reagent \geq
78 99.5%, and Hexadecyltrimethoxysilane (HDTS) technical grade \geq 85% were supplied by Sigma-Aldrich.
79 Low-Density Polyethylene (LDPE) pellets were supplied by Braskem with melt flow index of 1.7 g/10
80 min.

81 2.2 Functionalization

82 The functionalization process was performed using an adaptation of the method employed by Nguyen et
83 al. [20], in which a suitable amount of TiO_2 nanoparticles was added into ethanol solution; the dispersion
84 was subjected to sonication for 3 (10 min) cycles with a 5 minutes rest. Subsequently, the dispersion was
85 stirred to achieve a temperature of 65°C. Once the desired temperature was reached, the coupling agent
86 (HDTS) was dosed drop-by-drop according to the desired degree of functionalization (Table 1). The
87 reaction temperature increased to 78°C and refluxed for 3 h. The nanoparticles were recovered by
88 filtration and washed with ethanol to remove the unreacted coupling agent. Finally, the particles were
89 dried in a vacuum oven at 80°C for 12 h.

90 Table 1.
91 Composition of the reaction medium for functionalization

Sample ID	<i>EtOH</i> (wt %)	<i>TiO₂</i> (wt %)	<i>HDTS</i> (wt%)
TiO ₂	99	1	0
TiO ₂ FN-1	98.9	1	0.1
TiO ₂ FN-2	98.5	1	0.5

92

93 2.3 Characterization of nanoparticles

94 Three different analyses were performed to characterize the nanoparticles; the compatibility test; Infrared
95 Spectroscopy (FT-IR) and Thermogravimetric Analysis (TGA). The compatibility test was performed
96 using two solvents: deionized water and hexane. Unfunctionalized TiO₂, TiO₂ FN-1, and TiO₂ FN-2
97 nanoparticles were added to each solvent at a ratio of 0.1 g of nanoparticles per 10 mL of solvent. The
98 samples were stirred vigorously and left to rest for 20 minutes; dispersion could be observed afterwards.
99 Infrared spectroscopy (FT-IR-Affinity Shimadzu) was utilized to determine the degree of
100 functionalization; the different samples were subjected to a washing process and then exposed to a beam
101 of IR light. The washing process comprised the removal of the molecule's functionalizing agent. The
102 functionalized particles were filtered on a Whatman 40 paper, and then 100 mL of ethanol were added per
103 gram of sample; this process was performed in triplicate until the unreacted molecule's functionalizing
104 agent was removed from the sample, having dissolved in the alcohol solution. Last, Thermogravimetric
105 Analysis was carried out to determine weight loss using TGA-50 Shimadzu at a heating rate of 10°C/min
106 in air. The functionalizing agent content was determined by the following equation [22]:

$$n_f = 10^6 \frac{\Delta m_s}{m_f S_s MW_{silane}}$$

107 where n_f is the functionalizing agent content ($\mu\text{mol}/\text{m}^2$), Δm_s is the HDTS weight gain for the TiO₂ (g)
108 and measurement in TGA, m_s is the mass of the TiO₂ (g), S_s is the specific area of the TiO₂ (m^2/g), and
109 MW_{silane} is the molecular weight of the bonded silane molecule (g/mol). In this work, the molecular
110 weight of HDTS is 325 g / mol, considering a monodentate bond at the particle surface.

111 2.4 Preparation of the nanocomposite

112 The preparation of nanocomposites consists of mixing polymer pellets at a concentration 3% by the
113 weight of the nanoparticles; three samples were processed: one with unfunctionalized nanoparticles, and
114 two with functionalized nanoparticles at a concentration of TiO₂ FN-1 and TiO₂ FN-2 of coupling agent,
115 respectively. The mixing process was carried out in a turbomixer at 1,000 rpm for 2 min to prevent
116 overheating. After mixing, the different samples were extruded in a co-rotating twin screw extruder with
117 two intensive areas of mixed brand Rondol (L/D = 25:1) to obtain pellets (Table 2). The extrusion process
118 was performed employing the following temperature profile: 145; 185; 185; 195 and 200°C. The pellets

119 were processed in a hydraulic hot-press (Carver Press-8 Tons, 190°C) to obtain nanocomposite films of
 120 0.4 mm thickness. The concentration of nanoparticles in the polymer utilized in this study was determined
 121 considering that Daneshpayeh and collaborators in 2016 conducted an optimized concentration of TiO₂ in
 122 a polypropylene matrix to improve the mechanical properties, where the highest tensile strength is
 123 obtained at a concentration of 3% by weight [23].

124 Table 2. The film's composition processed under the same conditions

Sample ID	LDPE (%)	Nanoadditive (%)	Type (Nanoadditive)
LDPE	100	0	None
LDPE-TiO ₂	97	3	TiO ₂
LDPE-TiO ₂ FN-1	97	3	TiO ₂ FN-1
LDPE-TiO ₂ FN-2	97	3	TiO ₂ FN-2

125

126 2.5 Characterization of the nanocomposite

127 Four techniques were employed to characterize the nanocomposite samples. First, Differential Scanning
 128 Calorimetry (DSC) was performed under a heating rate of 10°C/min from a range of 30°-550°C (DSC Q
 129 200; TA Instruments). The crystallinity degree was estimated using $W_c = \Delta H_f / \Delta H^\circ$, where ΔH_f is the
 130 heat of fusion obtained after integrating the area under the melting curve and $\Delta H^\circ = 209$ J/g is the
 131 reference heat of fusion for LDPE in the first run. To perform the remaining other characterization
 132 techniques, the films (0.4 mm thick and 2 cm²) were exposed to UV radiation in a QUV Accelerated
 133 Weathering Tester (340 nm, I:0.5 W/m²; Q-Lab) for 250 h. Every 50 h, the samples were removed to
 134 analyze them by gravimetry and FTIR. To determine weight loss by gravimetric analysis, the irradiated
 135 films were washed with water and ethanol and then dried at 100°C for 2 hours before weighing the
 136 sample. Finally, after the 250 hours of exposure in the QUV, a Scanning Electron Microscope (SEM,
 137 NANOSEM 200-FEI) was used to observe the surface morphologies of the samples.

138 3. Results

139 3.1 FT-IR-Nanoparticles

140 Figure 1 depicts the FT-IR spectra for three different samples as follows: a) sample TiO₂ FN-2; b) sample
 141 TiO₂ FN-1; c) non-functionalized titanium dioxide and, d) the functionalizing agent is included (HDTs),
 142 which exhibits the characteristic bands of the aliphatic chain present (absorption bands 2,921, 2,852,
 143 1,465 and 721 cm⁻¹). With regard to sample (a), the related OH groups' band (3,700-3,000 cm⁻¹) which is
 144 lower in intensity with respect to the band for the sample (b), it demonstrated that a greater degree of
 145 functionalization because the OH group was partly substituted by the functionalizing agent. Additionally,
 146 it is possible to observe an increase in the intensity of the band corresponding to the CH vibrations with a

147 wave number of 2,921 and 2,951 cm^{-1} , of the aliphatic-chain methyls and methylenes to the aliphatic
148 chain to the sample (a), indicating that it contains a greater amount of functionalizing agent.

149 Figure 1.

150 3.2 Dispersion Test Nanoparticles

151 The compatibility test in water and hexane (Figure 2) illustrates the properties of compatibility in a polar
152 and non-polar medium, respectively. The compatibility test in water shows that the functionalized
153 particles behaved equally independent of their degree of functionalization, exhibiting no interaction with
154 the solvent, forming large agglomerates; some particles precipitated, while others were out of phase at the
155 surface, indicating its hydrophobic character. Contrariwise, it appears to disperse particles in hexane, as
156 they remained homogeneously dispersed, the agglomerates were practically null, and the particle size
157 allowed the particles to remain dispersed, indicating a good interaction with the non-polar medium.

158 Figure 2.

159 3.3 Thermogravimetric Analysis-Nanoparticles

160 In the TGA, the degree of functionalization is presented for each sample, where the difference in content
161 functionalizing agent is minimal (Figure 3). In the first case (TiO_2 FN-1) the total functionalizing agent
162 was added to the reaction (10% by weight) and only 2.2 % reacted with the surface of the particle
163 according to TGA, while for the second case (TiO_2 FN-2), where it was added at 50% by weight of the
164 functionalizing agent, the efficiency anchor revealed 2.9%. It is important to consider that the surface
165 functionalization may be limited by the steric effect; once the first molecules begin to react on the
166 surface, 16-carbon aliphatic chain could prevent new molecules from reacting on the surface [24]. This is
167 consistent with the results of FT-IR, in which partial functionalization presenting evidence vibration
168 signals corresponding to O-H confirmed the presence of hydroxyl groups on the particle surface. TGA
169 and FT-IR showed that, after washing process, the particles were reacted at a low proportion with the
170 functionalizing agent (2.2 and 2.9 wt%), indicating saturation of the particle surface: possibly the same
171 functionalizing agent excess in the reaction medium, adds on the aliphatic chains anchored to the particle.
172 At the end of the synthesis process, all excess functionalizing agent was removed, leaving areas with
173 unreacted hydroxyl groups, where there were TiO_2 FN-1 and TiO_2 FN-2 contents of 1.38 $\mu\text{mol}/\text{m}^2$ and 1.8
174 $\mu\text{mol}/\text{m}^2$, respectively.

175 Figure 3.

176 3.4 Characterization-Nanocomposite

177 The Scanning Transmission Electron Microscopy (STEM) technique was employed to observe the size of
 178 agglomerates in the polymer matrix. This technique permits measurement of the particle size in each
 179 sample analyzed wherein the content of titanium dioxide is the same all three samples (3 wt%). Figure 4
 180 shows the images obtained for two nanocomposite thin films: the micrograph (a) corresponds to the
 181 nanocomposite with unfunctionalized TiO₂, and micrograph (b) corresponds to the compound LDPE-
 182 TiO₂FN-2. The results reveal that functionalization improves distribution of particles in the matrix.
 183 Likewise, the size of unfunctionalized is larger than that of functionalized TiO₂ particles; the sizes ranges
 184 were 100-700 nm and 30-100 nm, respectively.

185 Figure 4.

186 Characterization by Differential Scanning Calorimetry (DSC) (Table 3) indicated that the crystallinity of
 187 the nanocomposite is affected by the size and distribution of the agglomerates in the polymer matrix.
 188 Thus, the nanocomposite with higher crystallinity is the sample with the higher degree of
 189 functionalization. This can be explained by that particles act as nucleating agents, thus increasing the
 190 number of crystals in the polymer matrix.

191 Table 3. Differential Scanning Calorimetry (DSC) characterization of the nanocomposite

Sample	ΔH_m (J/g)	T_m	T_c	X_c (%) _{LDPE}
LDPE	91.91	111,30	95,27	2,78
LDPE-TiO ₂	104.43	110,93	95,23	3,40
LDPE-TiO ₂ FN-1	99.61	110,98	95,21	3,23
LDPE-TiO ₂ FN-2	141.47	113.45	93.95	5.08

192

193 The mechanism of degradation of polyethylene proposed by Liu describes the formation of carboxylic
 194 acids, peroxide, hydroxyl peroxide, ketones, and alcohols, which are evident in the appearance of the
 195 bands C=O of the carboxyl group in 1,710 cm⁻¹ [15,25]. To analyze the nanocomposite degradation, the
 196 methodology described by many authors was utilized, [20,26,27,6], which considers the signal of the
 197 carbonyl determined in 1,710 cm⁻¹ in proportion to the abundance of the vibrations of methylene CH
 198 bond in 1,475 cm⁻¹. Four different samples were exposed to UV radiation for 250 h; in the results
 199 presented in Figure 5, we may observe that the sample without the titanium dioxide has a lower index of
 200 remaining carbonyls samples, therefore demonstrating that photocatalytic oxidation had been carried out.
 201 In samples containing titanium dioxide, it is possible to observe a higher rate of carbonyls at all of the
 202 analysis times for samples possess a degree of functionalization. The sample with the highest number of
 203 oxidized species was the LDPE-TiO₂FN-2, this result indicating that the functionalizing agent (as noted in
 204 the analysis of STEM analysis) promoted the reduction of particle size and a more homogeneous

205 distribution, which increases the formation of the film's surface in order for it to present a greater surface
206 area.

207 Figure 5.

208 TGA demonstrated the weight loss for the different samples analyzed. The results presented in Figure 6
209 demonstrate that the weight of the polymer with no additive remains constant, whereas the nanocomposite
210 samples decrease in weight over time. Recalling that the real difference between functionalized
211 nanoparticles is actually 2.2 and 2.9 wt %, respectively, it is possible to observe the difference in photo-
212 oxidative capacity. While the results of FT-IR spectroscopy indicated that the functionalized
213 nanoparticles in the higher level have more oxidized groups, in terms of actual weight loss,
214 nanocomposite samples with unfunctionalized nanoparticles and particles with a lower degree presented
215 greater weight loss. The main advantages of having functionalized nanoparticles for the production of
216 polymer nanocomposites are , certainly, to improve the distribution of nanoparticles in the matrix,
217 generating degradation levels of 7 and 9% in weight loss compared with the 11% weight loss generated
218 by the unfunctionalized sample.

219 Figure 6.

220 The SEM micrographs registered present surface modification after UV radiation. In the case of the
221 nanocomposite containing unfunctionalized and functionalized nanoparticles, LDPE TiO₂ FN-1,
222 degradation is performed heterogeneously with visible damage above the surface. Contrariwise, LDPE
223 TiO₂ FN-2 presented a homogeneous surface degradation, as presented in Figure 7. Other studies have
224 demonstrated that the ability to degrade a nanocomposite is dependent on two factors: the concentration
225 of the photocatalytic nanomaterial in the polymer, and the intensity of the UV radiation [7]. However, this
226 study presents the importance of the degree of functionalization to improve nanoparticle dispersion and to
227 decrease particle size in the polymer to improve compatibility. In another investigation, where titanium
228 dioxide is coated with a carbon layer, it was determined that the ability of photocatalytic degradation also
229 depends on the size and thickness of the particle's coating. It also concludes that degradation begins from
230 the interface between the TiO₂ and polymer layer and subsequently, the damage extends throughout the
231 surface[19]. In cases in which the particles occupying a larger surface area between the particle and the
232 polymer decrease, heterogeneous surface damage relates with fragmentation of the polymer sections, yet
233 the detached part that loses contact with the photocatalytic agent could stop degradation. A smaller
234 particle size increases the surface area and also provides support by means of a functionalizing agent,

235 partially anchoring the particles in the polymer matrix and exhibiting further degradation, that latter
236 evidenced by the formation of more oxidized species, ensuring the measurement index of carbonyl, and
237 more homogeneously, as observed in the STEM images. In the results presented here, the samples
238 without nanoparticles began its degradation after 95 h, while the remainder of the samples began to lose
239 weight after 15 hours. By comparing the samples with nanoparticles loss, greater weight is presented in
240 the sample with unfunctionalized TiO₂; however, as discussed in the analysis of the carbonyl index, this is
241 the sample with the lowest abundance of oxidized species, providing evidence of surface-damage weight
242 loss without this referring to chemical degradation.

243 Figure 7.

244 **Conclusions**

245 Partial functionalization of TiO₂FN-1 and TiO₂FN-2 nanoparticles was conducted, which was evident by
246 means of the FT-IR spectra. Furthermore, TGA demonstrated that the actual degree of functionalization
247 was 2.2 and 2.9%, respectively. There was a nanocomposite with LDPE by extrusion with different
248 functionalized particles in which films were formed by compression. Functionalization improved particle
249 dispersibility and adhesion in the polymer, achieving smaller particle sizes compared with those of the
250 unfunctionalized sample.

251 According to the results obtained by the carbonyl index and SEM, it was determined that, in the case
252 where the dispersion is improved, oxidation and degradation are greater and homogeneous. However, in
253 the gravimetry analysis, it presents greater weight loss was represented in the sample containing
254 unfunctionalized nanoparticles. The latter relates with the detachment of polymer sections without these
255 being degrading, i.e., a heterogeneous degradation occurs, which was due to the low surface area of the
256 chain-breaking process that takes place in limited regions.

257

258 Acknowledgments

259 Our acknowledgements go to Nanotechnology Incubator of Nuevo Leon for the facilities provided to
260 carry out this work, and to the XPERTO Company for their support in the developing accelerated
261 degradation tests in a UV weathering chamber.

262 References

- 263 [1] X.U. Zhao, Z. Li, Y. Chen, L. Shi, Y. Zhu, Solid-phase photocatalytic degradation of
264 polyethylene plastic under UV and solar light irradiation, *J. Mol. Catal. A Chem.* 268 (2007)

- 265 101–106. doi:10.1016/j.molcata.2006.12.012.
- 266 [2] H.M. Moghaddam, M.H. Khoshtaghaza, A. Salimi, M. Barzegar, The TiO₂–Clay-LDPE
267 Nanocomposite Packaging Films: Investigation on the Structure and Physicomechanical
268 Properties, *Polym. Plast. Technol. Eng.* 53 (2014) 1759–1767.
269 doi:10.1080/03602559.2014.919647.
- 270 [3] X. Zhao, Z. Li, Y. Chen, L. Shi, Y. Zhu, Enhancement of photocatalytic degradation of
271 polyethylene plastic with CuPc modified TiO₂ photocatalyst under solar light irradiation, *Appl.*
272 *Surf. Sci.* 254 (2008) 1825–1829. doi:10.1016/j.apsusc.2007.07.154.
- 273 [4] R.T. Thomas, V. Nair, N. Sandhyarani, TiO₂ nanoparticle assisted solid phase photocatalytic
274 degradation of polythene film: A mechanistic investigation, *Colloids Surfaces A Physicochem.*
275 *Eng. Asp.* 422 (2013) 1–9. doi:10.1016/j.colsurfa.2013.01.017.
- 276 [5] R.E. Day, The role of titanium dioxide pigments in the degradation and stabilisation of polymers
277 in the plastics industry, *Polym. Degrad. Stab.* 29 (1990) 73–92. doi:10.1016/0141-
278 3910(90)90023-Z.
- 279 [6] T. Manangan, S. Shawaphun, D. Sangsansir, Nano-Sized Titanium Dioxides as Photo-Catalysts
280 in Degradation of Polyethylene and Polypropylene Packagings, 1 (2010) 14–20.
- 281 [7] L. Zan, W. Fa, S. Wang, Novel photodegradable low-density polyethylene-TiO₂ nanocomposite
282 film., *Environ. Sci. Technol.* 40 (2006) 1681–5. doi:10.1021/es051173x.
- 283 [8] S. Singh, H. Mahalingam, P.K. Singh, Polymer-supported titanium dioxide photocatalysts for
284 environmental remediation: A review, *Appl. Catal. A Gen.* 462-463 (2013) 178–195.
285 doi:10.1016/j.apcata.2013.04.039.
- 286 [9] M. A Salem, Mechanical Properties of UV-Irradiated Low-Density Polyethylene Films
287 Formulated With Carbon Black and Titanium Dioxide, *Egypt. J. Sol.* 24 (2001) 141–150.
- 288 [10] C. Jin, P. A. Christensen, T. A. Egerton, E.J. Lawson, J.R. White, Rapid measurement of polymer
289 photo-degradation by FTIR spectrometry of evolved carbon dioxide, *Polym. Degrad. Stab.* 91
290 (2006) 1086–1096. doi:10.1016/j.polymdegradstab.2005.07.011.
- 291 [11] R. Yang, P. A. Christensen, T. A. Egerton, J.R. White, Degradation products formed during UV
292 exposure of polyethylene–ZnO nano-composites, *Polym. Degrad. Stab.* 95 (2010) 1533–1541.

- 293 doi:10.1016/j.polymdegradstab.2010.06.010.
- 294 [12] M. Ratova, A. Mills, Antibacterial titania-based photocatalytic extruded plastic films, J.
295 Photochem. Photobiol. A Chem. 299 (2015) 159–165. doi:10.1016/j.jphotochem.2014.11.014.
- 296 [13] T.J. Kemp, R. A. McIntyre, Influence of transition metal-doped titanium (IV) dioxide on the
297 photodegradation of polystyrene, Polym. Degrad. Stab. 91 (2006) 3010–3019.
298 doi:10.1016/j.polymdegradstab.2006.08.005.
- 299 [14] H.M.C. De Azeredo, Antimicrobial nanostructures in food packaging, Trends Food Sci. Technol.
300 30 (2013) 56–69. doi:10.1016/j.tifs.2012.11.006.
- 301 [15] Z. Liu, J. Jin, S. Chen, J. Zhang, Effect of crystal form and particle size of titanium dioxide on the
302 photodegradation behaviour of ethylene-vinyl acetate copolymer/low density polyethylene
303 composite, Polym. Degrad. Stab. 96 (2011) 43–50. doi:10.1016/j.polymdegradstab.2010.11.010.
- 304 [16] F. Magalhães, F.C.C. Moura, R.M. Lago, TiO₂/LDPE composites: A new floating photocatalyst
305 for solar degradation of organic contaminants, Desalination. 276 (2011) 266–271.
306 doi:10.1016/j.desal.2011.03.061.
- 307 [17] J. Velásquez, S. Valencia, L. Rios, G. Restrepo, J. Marín, Characterization and photocatalytic
308 evaluation of polypropylene and polyethylene pellets coated with P25 TiO₂ using the controlled-
309 temperature embedding method, Chem. Eng. J. 203 (2012) 398–405.
310 doi:10.1016/j.cej.2012.07.068.
- 311 [18] L. Reijnders, The release of TiO₂ and SiO₂ nanoparticles from nanocomposites, Polym. Degrad.
312 Stab. 94 (2009) 873–876. doi:10.1016/j.polymdegradstab.2009.02.005.
- 313 [19] M.M. Kamrannejad, A. Hasanzadeh, N. Nosoudi, L. Mai, A.A. Babaluo, H. Ave, Photocatalytic
314 Degradation of Polypropylene / TiO₂ Nano-composites, 17 (2014) 1039–1046.
- 315 [20] V.G. Nguyen, H. Thai, D.H. Mai, H.T. Tran, D.L. Tran, M.T. Vu, Effect of titanium dioxide on
316 the properties of polyethylene/TiO₂ nanocomposites, Compos. Part B Eng. 45 (2013) 1192–1198.
317 doi:10.1016/j.compositesb.2012.09.058.
- 318 [21] R. Tomovska, V. Daniloska, J.M. Asua, Surface modification of TiO₂ nanoparticles via
319 photocatalitically induced reaction: Influence of functionality of silane coupling agent, Appl. Surf.
320 Sci. 264 (2013) 670–673. doi:10.1016/j.apsusc.2012.10.091.

- 321 [22] S. Barus, M. Zanetti, M. Lazzari, L. Costa, Preparation of polymeric hybrid nanocomposites
322 based on PE and nanosilica, *Polymer (Guildf)*. 50 (2009) 2595–2600.
323 doi:10.1016/j.polymer.2009.04.012.
- 324 [23] S. Daneshpayeh, F. Ashenai Ghasemi, I. Ghasemi, M. Ayaz, Predicting of mechanical properties
325 of PP/LLDPE/TiO₂ nano-composites by response surface methodology, *Compos. Part B Eng.* 84
326 (2016) 109–120. doi:10.1016/j.compositesb.2015.08.075.
- 327 [24] S.P. Pujari, L. Scheres, A.T.M. Marcelis, H. Zuilhof, Covalent surface modification of oxide
328 surfaces., *Angew. Chem. Int. Ed. Engl.* 53 (2014) 6322–56. doi:10.1002/anie.201306709.
- 329 [25] I. Grigoriadou, K.M. Paraskevopoulos, K. Chrissafis, E. Pavlidou, T.G. Stamkopoulos, D.
330 Bikiaris, Effect of different nanoparticles on HDPE UV stability, *Polym. Degrad. Stab.* 96 (2011)
331 151–163. doi:10.1016/j.polymdegradstab.2010.10.001.
- 332 [26] S. Shawaphun, T. Manangan, S. Wacharawichanant, Thermo- and Photo- Degradation of LDPE
333 and PP Films Using Metal Oxides as Catalysts, *Funct. Sens. Mater.* 93-94 (2010) 505–508.
334 doi:DOI 10.4028/www.scientific.net/AMR.93-94.505.
- 335 [27] E. Yousif, A. Hameed, Synthesis and Photostability Study of Some Modified Poly (vinyl
336 chloride) Containing Pendant Benzothiazole and Benzimidazole Ring, (2010) 65–80.
337

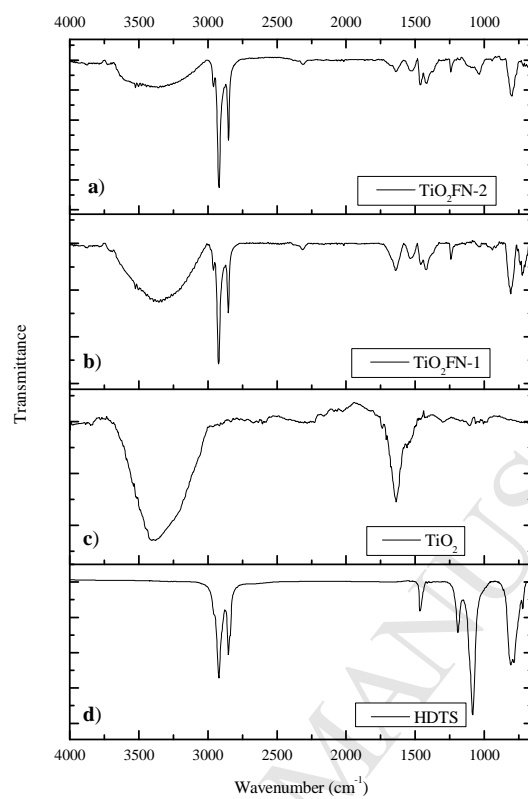


Figure 1. FT-IR Titanium dioxide nanoparticles (TiO_2), Hexadecyltrimethoxysilane (HDTS), functionalized nanoparticles (TiO_2 FN-1 and TiO_2 FN-2).

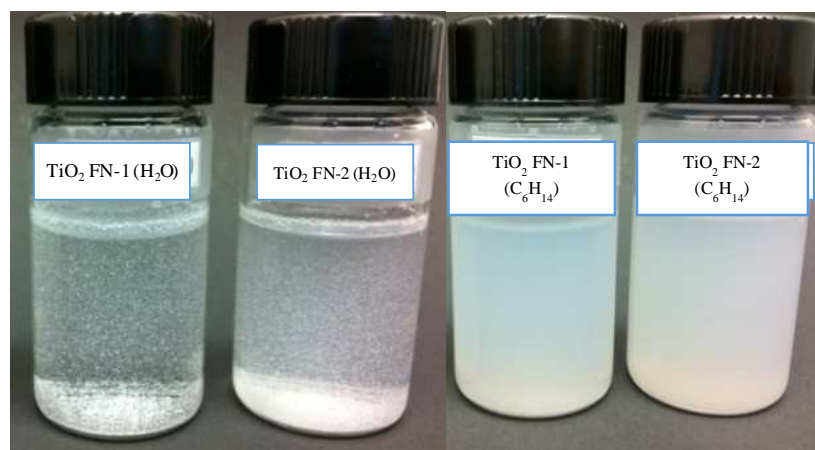


Figure 2. Compatibility test: particle aggregates in water(left) and dispersed particles in hexane(right).

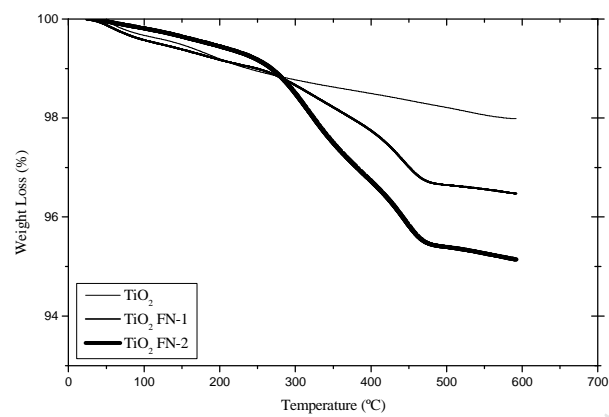


Figure 3. Thermogravimetric Analysis. Titanium dioxide unfunctionalized (TiO_2), titanium dioxide functionalized ($\text{TiO}_2\text{FN-1}$ and $\text{TiO}_2\text{FN-2}$).

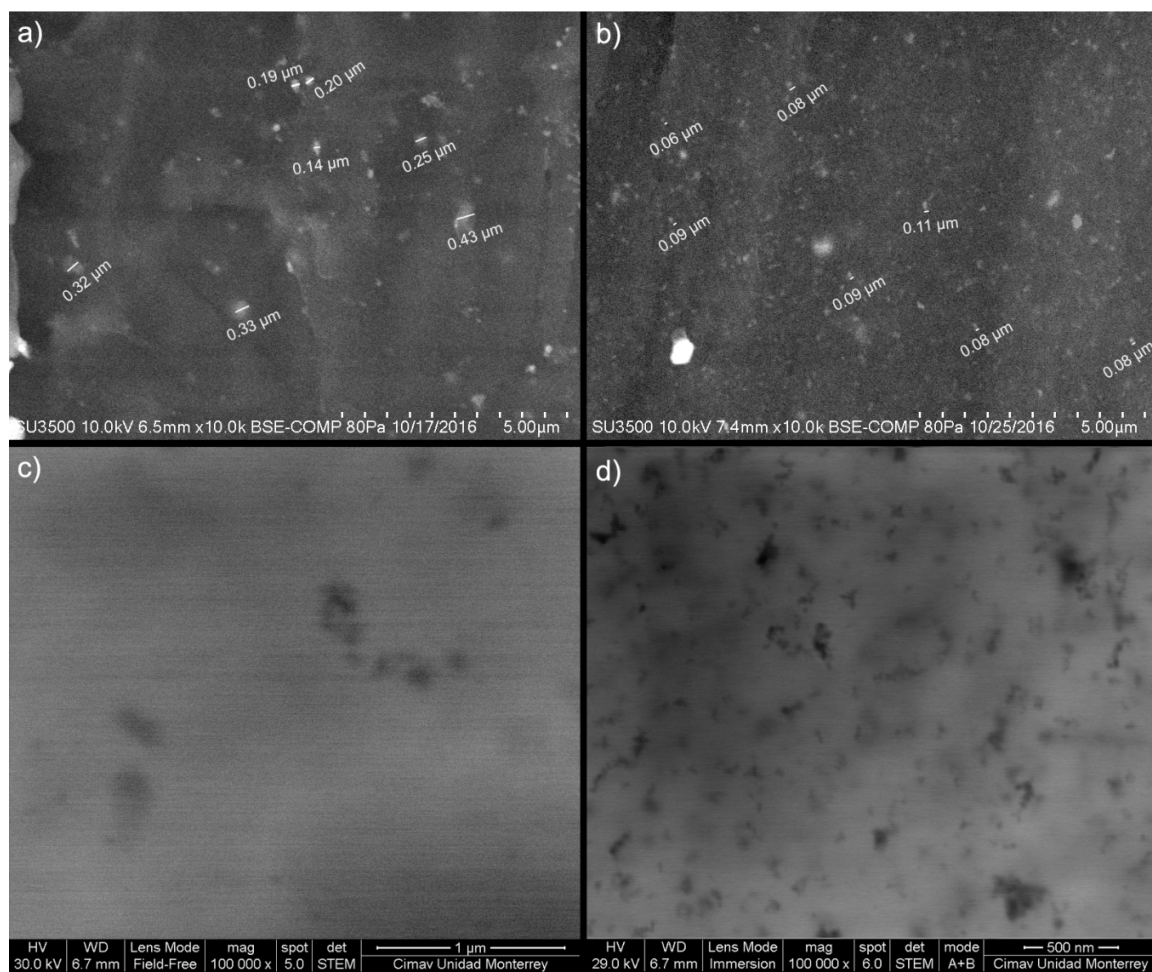


Figure 4. Nanocomposite LDPE-TiO₂ (a-SEM, c-STEM), Nanocomposite LDPE-TiO₂FN-2 (b-SEM, d-STEM).

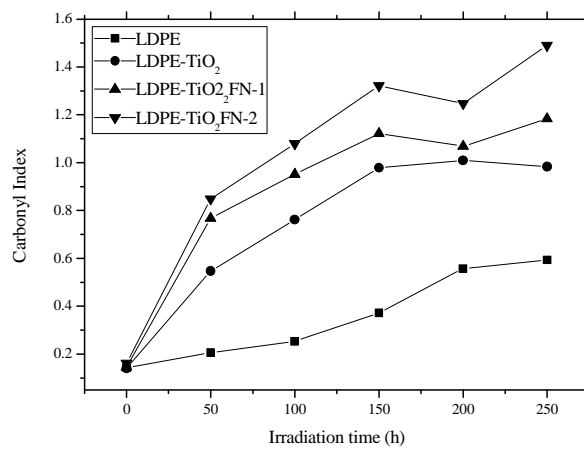


Figure 5. FT-IR Analysis-Carbonyl Index

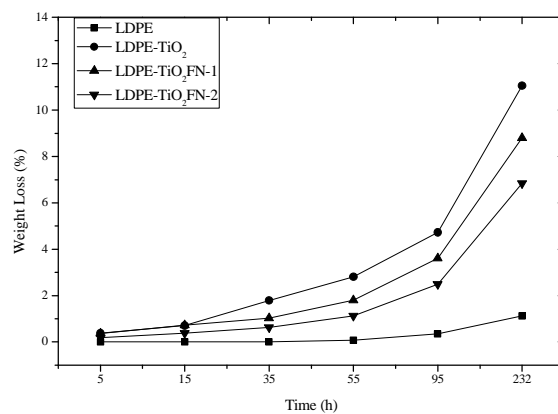


Figure 6. Gravimetry. LDPE (■), TiO₂ wt. (●), TiO₂FN-1 (▲), TiO₂FN-2 (▼).

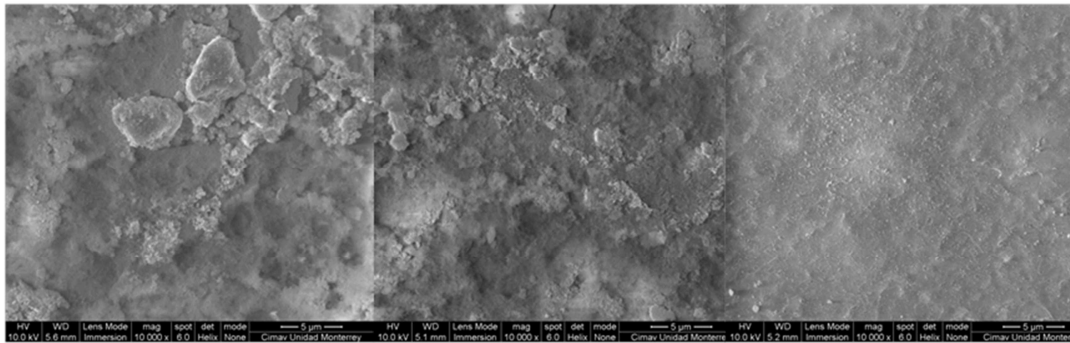


Figure 7. SEM- TiO_2 (left), $\text{TiO}_2\text{FN-1}$. (middle), $\text{TiO}_2\text{FN-2}$ (right).